Biochemical Pharmacology, Vol. 39, No. 3, pp. 445–453, 1990.
Printed in Great Britain.

0006-2952/90 $3.00 + 0.00
Pergamon Press plc

PURIFICATION AND PROPERTIES OF ALDOSE REDUCTASE AND ALDEHYDE REDUCTASE FROM EHS TUMOR CELLS

TSUYOSHI TANIMOTO, SANAI SATO and PETER F. KADOR*
National Eye Institute, National Institutes of Health, Bethesda, MD 20892, U.S.A.

(*Received* 5 *July* 1988; *accepted* 10 *July* 1989)

Abstract—Engelbreth–Holm–Swarm (EHS) tumor cells were utilized as a model for investigating the production of basement membrane components. These cells contain two immunologically distinct NADPH-dependent reductases, aldose reductase (EC 1.1.1.21) and aldehyde reductase (EC 1.1.1.2), which were purified to apparent homogeneity by a combination of procedures which included ammonium sulfate fractionation, Sephadex G-75 gel filtration, Matrex Gel Orange A affinity chromatography, and chromatofocusing on Pharmacia Mono P.

The molecular weights of aldose and aldehyde reductases were estimated to be 38K and 40K, respectively, by sodium dodecyl sulfate–polyacrylamide gel electrophoresis. Substrate specificity studies showed that both enzymes were capable of reducing a variety of aldehydes to their respective alcohols; however, only aldehyde reductase oxidized L-gulonic acid. Surprisingly, both enzymes showed similar reactivities with D-glucose and D-galactose, suggesting that both aldose and aldehyde reductases may contribute to sorbitol production in the EHS tumor cell. The activities of both enzymes were increased by the presence of sulfate ion, but chloride ion decreased the activity of aldose reductase. Both aldose and aldehyde reductases were inhibited by a series of structurally diverse aldose reductase inhibitors.

The enzyme aldose reductase (alditol:$NADP^+$ oxidoreductase, EC 1.1.1.21) has been implicated in the pathogenesis of several diabetic complications including cataracts, retinopathy, corneal abnormalities, neuropathy and possibly nephropathy [1]. Retinal capillary basement membrane thickening, a characteristic tissue alteration in diabetes, has been linked experimentally to aldose reductase in both diabetic and galactose-fed rats, and this thickening can be prevented by the administration of several structurally diverse aldose reductase inhibitors [2–5]. Since the small amounts of basement membrane and basement membrane producing tissues available from retinal capillaries make the elucidation of the apparent role of aldose reductase in this biochemical process difficult, we have employed the Engelbreth–Holm–Swarm (EHS) tumor as a model system for basement membrane production. These tumor cells have been reported to be a good source for basement membrane products [6].

In initial investigations, polyol production has been observed to occur in EHS tumor cells, and enzymatic analysis of partially purified enzyme from tumor tissue indicates the presence of an NADPH-utilizing reductase with a substrate profile consistent with aldose reductase [7]. Interestingly, biphasic kinetics similar to those reported for diabetic tissues [8, 9], were observed with this crude tissue. Therefore, in order to study the kinetics and properties of EHS tumor aldose reductase in more detail, the purification of aldose reductase from EHS tumor cells was investigated. Presently, two NADPH-reductases have been isolated from these tumor cells with properties corresponding to both aldose reductase and aldehyde reductase (EC 1.1.1.2).

* Send reprint requests to: Peter F. Kador, Ph.D., Building 10, Room 10B04, National Institutes of Health, Bethesda, MD 20892.

MATERIALS AND METHODS

Materials. Unless otherwise stated, all chemicals employed were of reagent grade quality or as previously reported [10]. Ammonium sulfate (enzyme grade) was obtained from Bethesda Research Laboratories, Inc. (Rockville, MD). NADPH and $NADP^+$ were obtained from Boehringer Mannheim (Indianapolis, IN). Sephadex G-75, Polybuffer 74 and Mono P for chromatofocusing, and molecular weight standards for sodium dodecyl sulfate–polyacrylamide gel electrophoresis (SDS–PAGE) and gel filtration were purchased from Pharmacia Fine Chemicals (Piscataway, NJ). Matrex Gel Orange A was obtained from the Amicon Corp. (Danvers, MA). All electrophoretic reagents were obtained from Bio-Rad Laboratories (Richmond, CA). Al 1576, sorbinil, tolrestat, M79175 and Ponalrestat (Statil) were donated by Alcon Laboratories (Fort Worth, TX); Pfizer Central Research (Groton, CT); Ayerst Central Research, Inc. (Princeton, NJ); Eisai Pharmaceutical Co. (Tokyo, Japan); and Stuart-ICI Americas (Wilmington, DE), respectively. EHS tumor tissue was obtained from C57BL mice implanted with the tumor as previously described [7] and stored frozen at −70°.

Enzyme assay. Reductase activity was assayed spectrophotometrically on a Gilford Response spectrophotometer by following the decrease in the absorption of NADPH at 340 nm over a 4-min period with DL-glyceraldehyde as substrate [11]. Dehydrogenase activity was assayed by following over a 4-

min period the increase in the absorption of NADPH when L-gulonate was used as substrate [12]. In the enzyme assay, each 1.0-mL cuvette contained 0.01 M Na^+K^+ phosphate buffer, pH 6.2, 0.3 mM NADPH or $NADP^+$, 10 mM substrate with/without inhibitor and adequate enzyme solution. Appropriate controls were employed to negate potential changes in the absorption of nucleotide and/or inhibitors at 340 nm in the absence of substrate. One unit of enzyme activity was defined as the activity consuming 1 nmol of NADPH/min at 22°. Kinetic calculations were conducted on the NIH PROPHET computer system, and IC_{50} calculations were conducted as described previously [13].

Protein determination. Protein was determined spectrophotometrically according to the method of Bradford [14].

Purification of aldose and aldehyde reductases from EHS tumor. All purification steps were carried out at 4°. In the initial extraction, 100 g of thawed EHS tumor material was homogenized with 300 mL of 20 mM phosphate buffer, pH 7.5, containing 0.7 mM EDTA and 5 mM β-mercaptoethanol, and the homogenate was centrifuged at 10,000 *g* for 15 min. The supernatent fluid was then fractionated with solid ammonium sulfate, and the precipitate obtained from a similar centrifugation of the 30–60% ammonium sulfate fraction was collected and dissolved in *ca.* 25 mL of the same phosphate buffer. One-half of this enzyme solution was then applied at a time to a Sephadex G-75 column (2.5 × 90 cm), and the protein mixture was eluted with the same phosphate buffer and collected in 150-drop fractions (*ca.* 10 mL). Fractions containing reductase activity were combined and applied to a column (2.5 × 15 cm) of Matrex Gel Orange A. The column was washed with 500 mL of the phosphate buffer followed by 200 mL of 10 mM imidazole buffer, pH 7.6, containing 1 mM β-mercaptoethanol. The enzymes were then eluted as a single peak from the affinity column with 0.1 mM NADPH dissolved in the same imidazole buffer and collected in 120-drop aliquots (*ca.* 8 mL). Finally, the enzyme fractions were chromatofocused on Pharmacia Mono P equilibrated with the imidazole buffer, pH 7.6, containing 1 mM β-mercaptoethanol and developed with 10-fold diluted Polybuffer 74 at the flow rate of 1 mL/min. The protein concentration of the eluent was monitored spectrophotometrically at 280 nm, and two main peaks, corresponding to aldehyde reductase and aldose reductase, were collected.

Preparation of rat lens aldose reductase and rat kidney aldehyde reductase. Both rat lens aldose reductase and rat kidney aldehyde reductase were purified as previously reported [11, 12].

Polyacrylamide gel electrophoresis. Sodium dodecyl sulfate–polyacrylamide gel electrophoresis (SDS–PAGE) was performed according to the method of Laemmli [15] using phosphorylase *b* (94K), bovine serum albumin (67K), ovalbumin (43K), carbonic anhydrase (30K), soybean trypsin inhibitor (20.1K) and α-lactalbumin (14.4K) as molecular weight standards. Native gel electrophoresis was performed on 12.5% acrylamide gel (PhastGel homogenous 12.5) with the Pharmacia PhastGel system. Proteins were stained with Coomassie blue.

Isoelectric focusing. Isoelectric focusing was performed on acrylamide gel (PhastGel IEF 3-9) with the Pharmacia PhastGel system. Proteins were visualized with Coomassie blue stain.

Molecular weight determination by gel filtration. Gel filtration for molecular weight determinations was performed by high pressure liquid chromatography (HPLC) on an UltraPac TSK-W2000 (LKB) column. The column, equilibrated with 20 mM phosphate buffer, pH 7.5, containing 0.3 M NaCl, was eluted with the same buffer at a flow rate of 0.5 mL/min, while protein concentrations were monitored spectrophotometrically at 280 nm. When crude sample was used, the elution peaks corresponding to aldose reductase and aldehyde reductase activity were confirmed by spectrophotometrically measuring the enzyme activity with DL-glyceraldehyde as substrate. Protein standards used for the calculation of molecular weights included bovine serum albumin (67K), ovalbumin (43K), carbonic anhydrase (30K) and chymotrypsinogen (25K).

Antibodies. Antibodies against purified aldose reductase and aldehyde reductase were raised in goats by three injections, at 2-week intervals, of 250 μg of the purified enzyme mixed with equal volumes of complete Freund's adjuvant. Double-immunodiffusion was performed on Ouchterlony plates.

Amino acid analysis. For determination of the amino acid composition, the purified enzymes were dialyzed thoroughly against water, lyophilized, and hydrolyzed *in vacuo* at 110° with 6 N HCl for 24, 48 and 72 hr. The hydrolysates were freed from HCl by drying in an evaporator and were then analyzed by the method of Spackman *et al.* [16]. Half-cystine and methionine were determined with a performic acid oxidized sample, and the contents of threonine and serine were extrapolated back to zero time. For valine and isoleucine, the values from the 72-hr hydrolysate were employed.

RESULTS

Two NADPH-dependent reductases, identified as aldose reductase and aldehyde reductase, were purified from EHS tumor tissue in the five steps summarized in Table 1. With either DL-glyceraldehyde or D-glucuronate as substrate, only a single peak of NADPH-dependent reductase activity was obtained after both gel filtration on Sephadex G-75 (Fig. 1) and affinity chromatography on Matrex Gel Orange A (Fig. 2). Subsequent chromatofocusing on Mono P of the enzyme fractions obtained from the Matrex Gel Orange A resulted in the appearance of two peaks of enzyme activity (Fig. 3). Each enzyme peak appeared as single line on SDS–PAGE (Fig. 4), native PAGE (Fig. 5) and isoelectric focusing (Fig. 6), suggesting that both enzymes were purified to apparent homogeneity. Moreover, each enzyme appeared distinct with respect to molecular weight and isoelectric point, and antibodies raised against protein from either peak failed to cross-react, indicating that both enzymes were immunologically distinct (Fig. 7). The more basic protein with a pI of 6.1 had an apparent molecular weight of 40K on

Table 1. Purification of aldose and aldehyde reductases from EHS tumor cells

Step	Total protein (mg)	Total activity (units)	Specific activity (units/mg)	Purification (fold)	Yield (%)
Homogenate	2743	6721	2.53	1.0	100
30–60% $(NH_4)_2SO_4$	1160	6686	5.64	2.3	99
Sephadex G-75	1163	6318	5.43	2.2	94
Matrex Gel Orange A	2.34	5036	2152	878	74
Mono P chromatofocusing					
ALR	0.387	2171	5611	2218	32.3
AR	0.865	995	1150	454	14.8

Based on 100 *g* of EHS tumor material. One unit of enzyme activity is defined as the activity consuming 1 nmol of NADPH/min at 22° with 10 mM DL-glyceraldehyde as substrate.

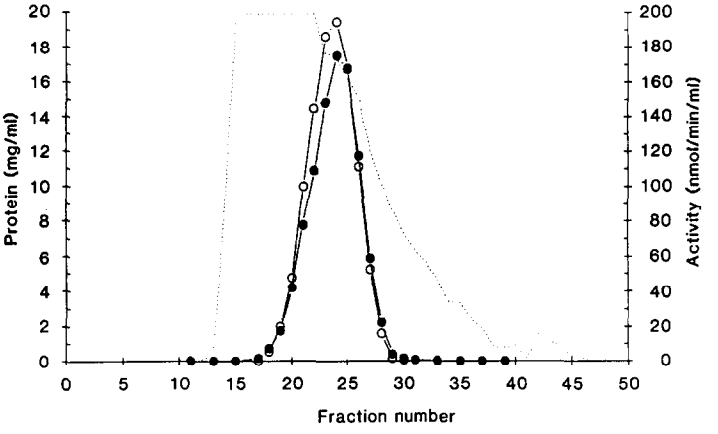

Fig. 1 Elution pattern obtained from gel filtration on Sephadex G-75 of EHS tumor cell extract after 30–60% ammonium sulfate fractionation. The dotted line indicates the protein concentration; closed and open circles indicate enzyme activity (nmol NADPH utilized/min/1 mL enzyme solution) with DL-glyceraldehyde and D-glucuronate as substrate respectively.

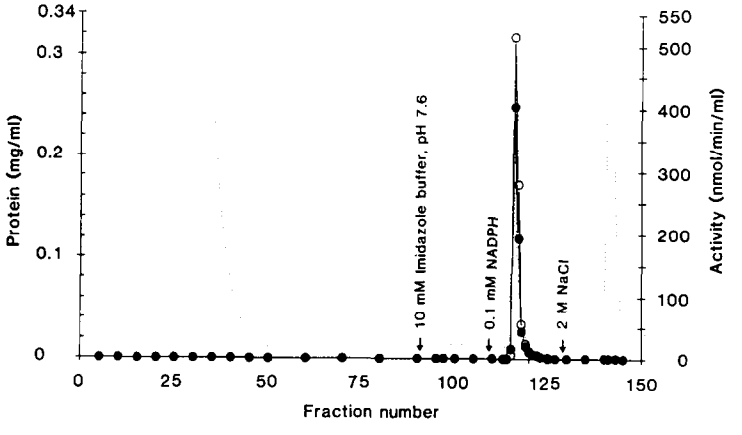

Fig. 2. Elution pattern for affinity chromatography on Matrex Gel Orange A of the enzyme fractions obtained by gel filtration on Sephadex G-75. The protein concentration is indicated by the dotted line; the enzyme activity (nmol NADPH utilized/min/1 mL enzyme solution) with DL-glyceraldehyde and D-glucuronate as substrate is indicated by closed and open circles respectively.

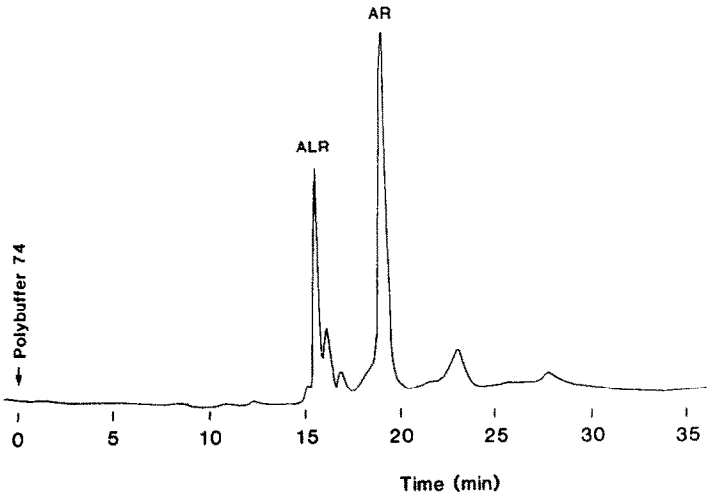

Fig. 3. Elution pattern obtained from chromatofocusing on Mono P of the single peak of enzyme activity eluted from the Matrex Gel Orange A column. The column was equilibrated with 10 mM imidazole-HCl buffer, pH 7.6, containing 1 mM β-mercaptoethanol, and elution was conducted at a flow rate of 1 mL/min with 10-fold diluted Polybuffer 74 containing 1 mM β-mercaptoethanol. The protein concentration of the eluent was monitored spectrophotometrically at 280 nm.

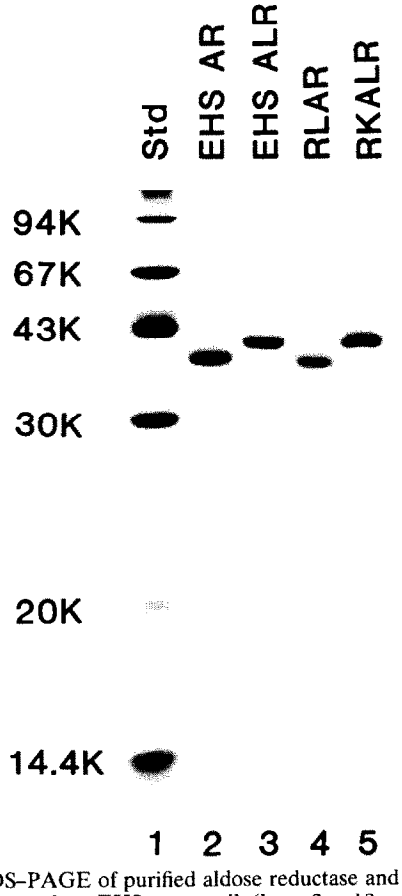

Fig. 4. SDS-PAGE of purified aldose reductase and aldehyde reductase from EHS tumor cells (lanes 2 and 3 respectively) compared to rat lens aldose reductase (lane 4) and rat kidney aldehyde reductase (lane 5). Molecular weight standards in lane 1 include phosphorylase *b* (94K), bovine serum albumin (67K), ovalbumin (43K), carbonic anhydrase (30K), soybean trypsin inhibitor (20.1K) and α-lactalbumin (14.4K).

SDS-PAGE and appeared to co-migrate with purified rat kidney aldehyde reductase (Fig. 4), whereas the more acidic protein, pI 5.6, had an apparent molecular weight of 38K and comigrated with rat lens aldose reductase. By gel filtration on TSK-W200

Fig. 5. Native PAGE of purified EHS tumor aldose reductase (lane 1) and aldehyde reductase (lane 2). Proteins were visualized with Coomassie blue stain.

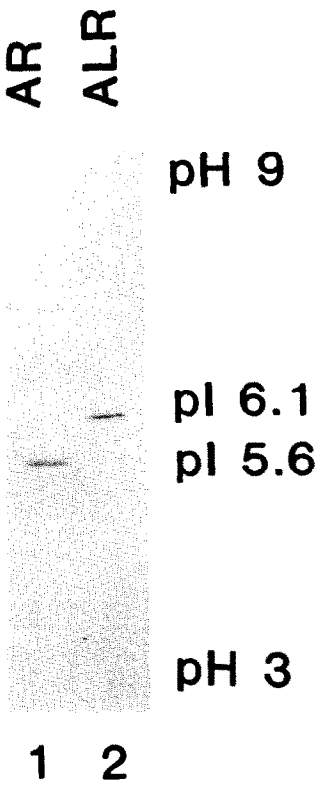

Fig. 6. Isoelectric focusing on acrylamide gel of the purified EHS tumor aldose reductase (lane 1) and aldehyde reductase (lane 2). The gel was stained with Coomassie blue.

each enzyme eluted as a single peak with a similar apparent molecular weight of 37K, indicating that both enzymes were monomers. Antibodies raised against the more basic peak also cross-reacted with rat kidney aldehyde reductase, whereas antibodies raised against the more acidic protein cross-reacted with rat lens aldose reductase. Similarly, antibodies raised against rat lens aldose reductase recognized the more acidic protein, while antibodies against rat kidney aldehyde reductase recognized both peaks.

A comparative study of substrate specificities was conducted on both enzyme fractions (Table 2). For reductase activity with NADPH, the lower molecular weight enzyme of pI 5.6 utilized substrate in the order *p*-nitrobenzaldehyde > DL-glyceraldehyde > D-glucuronate > D-xylose > D-galactose > D-glucose, whereas the higher molecular weight protein, pI 6.1, utilized substrate in the order *p*-nitrobenzaldehyde > DL-glyceraldehyde ≥ D-glucuronate > D-galactose > D-glucose > D-xylose. The more basic protein also utilized $NADP^+$ to oxidize L-gulonic acid to D-glucuronic acid, whereas the more acidic protein displayed only trace activity with 40 mM L-gulonate. Only linear kinetics were observed with either purified enzyme.

Based on substrate specificity profiles, the ability to oxidize L-gulonate, and immunological properties, the higher molecular weight protein of pI 6.1 was identified as aldehyde reductase and the slightly smaller protein of pI 5.6 was identified as aldose reductase. Activity responses to the presence of sulfate and chloride were also consistent with these assignments (Table 3). In the presence of 0.3 M ammonium sulfate, the activities of aldose reductase and aldehyde reductase increased 2.3 and 1.5 times. Similar activation was also observed in the presence of 0.3 M lithium sulfate. However, 0.1 M sodium chloride decreased the activity of aldose reductase by 25% while slightly increasing the activity of aldehyde reductase.

In general, the amino acid compositions of EHS tumor aldose reductase and aldehyde reductase were very similar (Table 4), though major differences were observed in serine, half-cystine and histidine. With the exception of serine, alanine and half-cystine in rat kidney aldehyde reductase, similarities were also observed in the comparison of the amino acid composition of EHS tumor aldehyde reductase to rat kidney aldehyde reductase. Similarly, with the exception of glycine, valine and leucine, the amino acid composition of rat lens aldose reductase closely matched that of EHS tumor aldose reductase.

Both purified enzymes from the EHS tumor cells were inhibited by the structurally diverse aldose reductase inhibitors 7-hydroxy-2-chromone carboxylic acid, Al 1576 (2,7-difluorospirofluorene-9,5′-imidazolidine-2′,4′-dione), sorbinil ((*S*)-6-fluorospiro [chroman-4,5′-imidazolidine]-2′,4′-dione), M79175 (2-methyl-6-fluorospiro-[chroman-4,5′-imidazolidine]-2′,4′-dione), tolrestat (*N*-[[5-trifluoromethyl)-6-methoxy-1-naphthalenyl]thioxomethyl]-*N*-methylglycine) and Ponalrestat (Statil, [(3-[4-bromo-2-fluorobenzyl]-4-oxo-3*H*-phthalazin-1-yl)-

Table 2. Substrate specificity of EHS tumor aldehyde and aldose reductases

	Aldehyde reductase		Aldose reductase	
Substrate	K_m* (mM)	% V_{max}	K_m* (mM)	% V_{max}
DL-Glyceraldehyde	3.0 ± 0.68	100.0	0.056 ± 0.007	100.0
D-Xylose	704 ± 25	5.4	22.8 ± 1.6	30.1
D-Glucose	166 ± 28	2.7	189 ± 15	3.8
D-Galactose	90.5 ± 20.4	4.5	53.9 ± 9.0	10.7
D-Glucuronate	3.1 ± 0.43	105.4	11.8 ± 1.2	25.5
L-Gulonate	8.0 ± 2.2	7.8	Trace at 40 mM	
p-Nitrobenzaldehyde	0.20 ± 0.015	120.9	0.0093 ± 0.0009	110.8

*Values are means ± SD, N = 3.

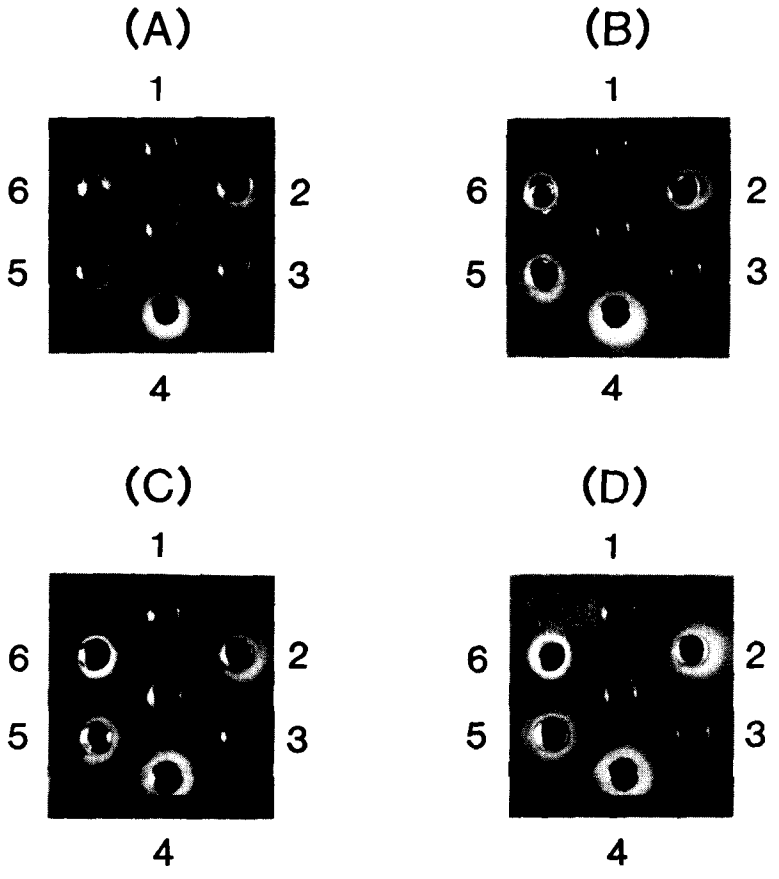

Fig. 7. Double-immunodiffusion on Ouchterlony plates illustrating the immunological relationship between purified EHS tumor aldose reductase and aldehyde reductase and rat lens aldose reductase and kidney aldehyde reductase. All plates contained EHS tumor aldose reductase in well 1, EHS tumor cell homogenate in wells 2 and 5, EHS aldehyde reductase in well 3, rat kidney aldehyde reductase in well 4, and rat lens aldose reductase in well 6. In (A) antibodies raised in goat against EHS aldose reductase were placed in the center well, while in (B) antibodies against EHS aldehyde reductase were employed. In (C) and (D) antibodies raised against rat lens aldose reductase and rat kidney aldehyde reductase were placed in each center well respectively.

acetic acid]), as summarized in Table 5. Aldose reductase was inhibited most strongly by tolrestat, which displayed an IC_{50} value of 1.7×10^{-8} M, while sorbinil with an IC_{50} of 3.2×10^{-5} M was the least effective inhibitor. The IC_{50} values for M79175, Ponalrestat, Al 1576 and 7-hydroxy-2-chromone carboxylic acid were 6.8×10^{-7}, 3.0×10^{-6}, 7.5×10^{-6} and 5.0×10^{-6} M respectively. On the other hand, aldehyde reductase was inhibited most strongly by Al 1576 and M79175 with IC_{50} values of 8.3×10^{-9} and 7.0×10^{-8} M respectively. All other compounds displayed IC_{50} values in the 3×10^{-6} M range.

DISCUSSION

Observations that aldose reductase inhibitors can

Table 3. Effect of salt on aldose and aldehyde reductase activity with DL-glyceraldehyde as substrate

	% Relative activity			
	Aldehyde reductase*		Aldose reductase*	
Salt	EHS	Rat kidney	EHS	Rat lens
None	100	100	100	100
0.3 M $(NH_4)_2SO_4$	152	144	233	206
0.3 M Li_2SO_4	142	137	165	166
0.1 M NaCl	117	111	75	80

* With 10 mM glyceraldehyde as substrate.

Table 4. Comparison of amino acid compositions of aldose and aldehyde reductases from EHS tumor versus rat lens aldose and kidney aldehyde reductases

	Number of residues/mol of enzyme			
	Aldehyde reductase		Aldose reductase	
Amino acid	EHS tumor	Rat kidney	EHS tumor	Rat lens
Asp	45	45	37	37
Thr	20	16	15	16
Ser	46	23	26	26
Glu	46	39	39	46
Pro	15	19	19	22
Gly	35	17	26	17
Ala	33	23	30	35
1/2 Cys	15	9	5	5
Val	45	50	47	56
Met	12	14	8	9
Ile	11	14	9	11
Leu	24	28	29	38
Tyr	7	10	9	11
Phe	7	9	7	7
His	7	8	14	9
Lys	15	21	15	16
Arg	12	11	17	11

prevent retinal capillary basement membrane thickening in both diabetic and galactose-fed animals have spurred interest in elucidating the biochemical role of aldose reductase in this process. Using EHS tumor cells as a model system for basement membrane production, we had observed previously that these cells produce galactitol when raised in galactose-fed mice and possess an NADPH-utilizing reductase with a substrate profile that is consistent with aldose reductase [7]. Purification studies now reveal that two distinct peaks of enzyme activity utilizing NADPH are present in these cells. Based on their ability to reduce a variety of aldehydes, oxidize gulonic acid and react to the presence of sulfate and chloride ions, these two peaks were identified as aldehyde reductase and aldose reductase. Aldehyde reductase and aldose reductase were purified to apparent homogeneity with approximately 2218- and 454-fold purification and 32 and 15% recovery respectively. Both purified enzymes are monomers and appeared on SDS–PAGE as single bands which comigrated with purified rat lens aldose reductase and rat kidney aldehyde reductase (Fig. 4).

Sephadex G-75 gel filtration studies with partially purified enzyme subjected to ammonium sulfate fractionation indicated an elution pattern of reductase activity identical to that observed for crude tumor cell homogenate (Fig. 8). This observation indicates that the EHS tumor enzymes were not generated by ammonium sulfate induced cleavage of a larger protein as suggested by Srivastava *et al.* [17]. Moreover, the immunological distinctness of each enzyme, indicated by the failure of antibodies raised against the 38K or 40K polypeptide to cross-react with the 40K and 38K polypeptide, respectively, suggests that the 38K enzyme is not a cleavage product of the 40K enzyme. Antibodies against EHS tumor aldose reductase also cross-reacted with rat lens aldose reductase, whereas antibodies against EHS tumor aldehyde reductase cross-reacted with rat kidney aldehyde reductase. In addition, antibodies raised against rat lens aldose reductase also cross-reacted

Table 5. Inhibition of aldose and aldehyde reductases from EHS tumor by aldose reductase inhibitors

	IC_{50} (μM)	
Inhibitor	Aldehyde reductase	Aldose reductase
7-Hydroxy-2-chromone carboxylic acid	2.8 ± 0.01	5.0 ± 0.28
Al 1576	0.0083 ± 0.0005	7.5 ± 0.60
Sorbinil	2.9 ± 0.05	32 ± 2.6
M79175	0.07 ± 0.005	0.68 ± 0.03
Tolrestat	2.6 ± 0.16	0.017 ± 0.0004
Ponalrestat	3.0 ± 0.02	3.0 ± 0.11

Values are means ± SD, N = 3–5.

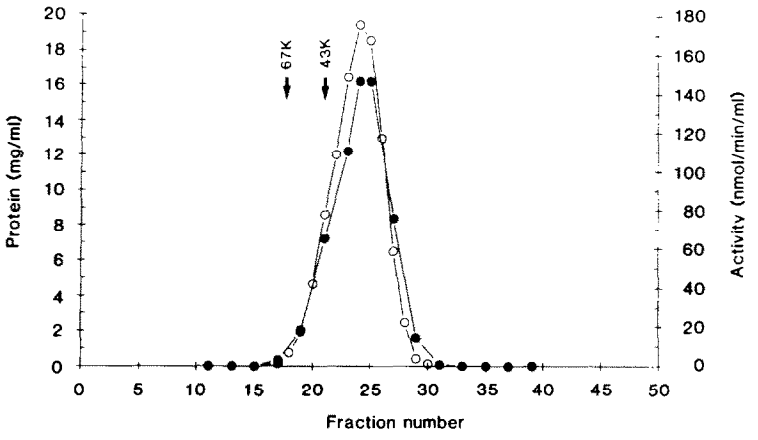

Fig. 8. Elution pattern of enzyme activity (nmol NADPH utilized/min/1 mL enzyme solution with DL-glyceraldehyde as substrate) obtained from gel filtration on Sephadex G-75 of crude EHS tumor homogenate (closed circles) versus EHS tumor cell extract after 30–60% ammonium sulfate fractionation (open circles). Arrows respresent protein peaks obtained with bovine serum albumin (67K) and ovalbumin (43K).

with EHS tumor aldose reductase. Interestingly, antibodies against rat kidney aldehyde reductase recognized both EHS tumor aldehyde reductase and aldose reductase but not rat lens aldose reductase (Fig. 7).

Kinetic studies also confirm the presence of two distinct enzymes in EHS tumor cells. Studies with partially purified enzyme under saturating conditions [7] or crude tumor homogenate, as illustrated in Fig. 9, indicate the presence of biphasic Lineweaver–Burk plots from which two K_m values can be estimated. These "high" and "low" K_m values closely correspond to the individual K_m values obtained for purified aldehyde reductase and aldose reductase (Fig. 10), indicating that the biphasic kinetics are composites of the two individual enzymes. The purified enzymes also showed significant differences in their susceptibility to be inhibited by aldose reductase inhibitors. Greatest selectivity, with over a 900-fold difference in the IC_{50} values for aldehyde reductase, was observed with Al 1576, while over a 150-fold difference for aldose reductase was displayed by tolrestat. Essentially equal inhibition of both enzymes was observed with Ponalrestat and 7-hydroxy-2-chromone carboxylic acid.

Although the purified aldose reductase and aldehyde reductase display several similarities to rat lens aldose reductase and kidney aldehyde reductase, respectively, the EHS tumor cell enzymes, unlike their rat enzyme counterparts, displayed a similar affinity for D-glucose and D-galactose. This suggests that both aldose and aldehyde reductases may con-

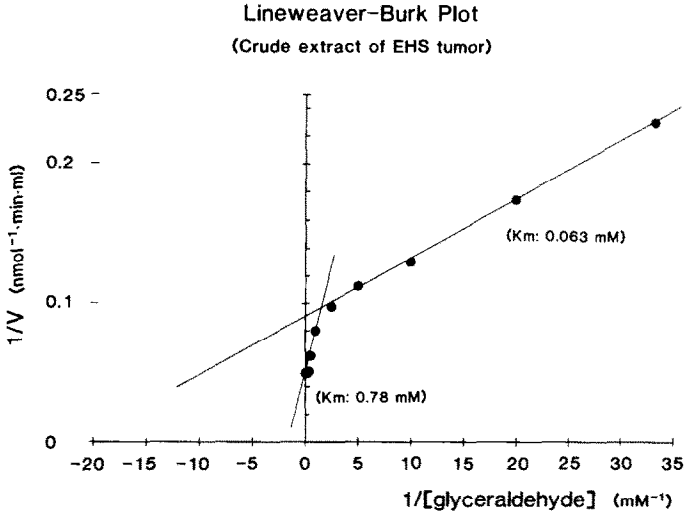

Fig. 9. Lineweaver–Burk plot of the NADPH-dependent reductase activity from crude extract of EHS tumor, illustrating the biphasic kinetics obtained with DL-glyceraldehyde as substrate.

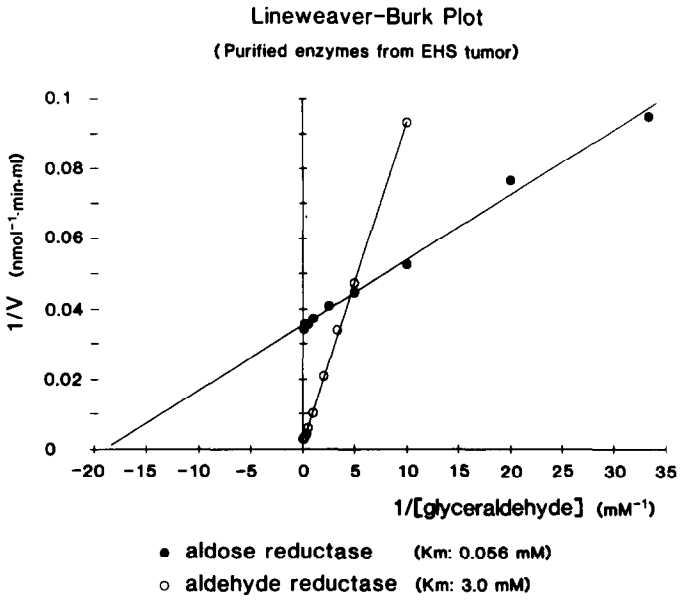

Fig. 10. Lineweaver–Burk plots of purified EHS tumor aldose reductase (closed circles) and aldehyde reductase (open circles) illustrating the linear kinetics observed with each enzyme with DL-glyceraldehyde as substrate.

tribute to sorbitol production in the EHS tumor cell. Because of the apparent selectivity of the aldose reductase inhibitors Al 1576 and tolrestat for aldehyde reductase and aldose reductase, respectively, these inhibitors should serve as useful tools in elucidating the apparent role of these enzymes in the EHS tumor cells.

REFERENCES

1. Kador PF, Pharmacology of aldose reductase inhibitors. *Med Res Rev* **8**: 325–352, 1988.
2. Robison WG Jr, Kador PF and Kinoshita JH, Basement membrane thickening by galactosemia prevented with aldose reductase inhibitor. *Science* **221**: 1177–1179, 1983.
3. Frank RN, Keirn RJ, Kennedy A and Frank KW, Galactose-induced retinal capillary basement membrane thickening: prevention by sorbinil. *Invest Ophthalmol Vis Sci* **24**: 1519–1524, 1983.
4. Robison WG Jr, Kador PF, Akagi Y, Kinoshita JH, Gonzalez R and Dvornik D, Prevention of basement membrane thickening in retinal capillaries by a novel aldose reductase inhibitor, tolrestat. *Diabetes* **35**: 295–299, 1986.
5. Stribling D, Mirrless DJ, Harrison HE and Earl DCN, Properties of ICI 128436 [(3,4-bromo-2-fluorobenzyl)-4-oxo-3*H*-phthalazin-1-ylacetic acid], a novel aldose reductase, EC 1.1.1.21, inhibitor and its effects on diabetic complications in the rat. *Metab Clin Exp* **34**: 336–344, 1985.
6. Rohrbach DH, Ledbetter SR, Wagner CW, Horigan EA, Hassell JR and Martin GR, Use of the EHS tumor as a model for studying basement membrane synthesis in normal and diabetic mice. In: *Methods in Diabetes Research* (Eds. Larner J and Pohl SL), Vol. 1C, pp. 399–418. John Wiley, New York, 1985.
7. Kador PF, Terubayashi H, Millen J and Kinoshita JH, The role of aldose reductase in the development of diabetic complications. In: *Polyol Pathway and Its Role in Diabetic Complications* (Eds. Sakamoto N, Kinoshita JH, Kador PF and Hotta N), pp. 20–31. Elsevier, Amsterdam, 1988.
8. Das B and Srivastava SK, Activation of aldose reductase from human tissues. *Diabetes* **34**: 1145–1151, 1985.
9. Srivastava SK, Ansari NH, Hair GA, Awasthi S and Das B, Activation of human erythrocytes, brain, aorta, muscle and ocular tissue aldose reductase. *Metabolism* **35**: 114–118, 1986.
10. Kador PF, Carper DH and Kinoshita JH, Rapid purification of human placental aldose reductase. *Anal Biochem* **114**: 53–58, 1981.
11. Shiono T, Sato S, Reddy VN, Kador PF and Kinoshita JH, Purification and properties of rat lens aldose reductase. *Prog Clin Biol Res* **232**: 317–324, 1987.
12. Sato S, Kador PF and Kinoshita JH, Rat kidney aldehyde reductase: Purification and comparison with rat lens aldose reductase. In: *Polyol Pathway and Its Role in Diabetic Complications* (Eds. Sakamoto N, Kinoshita JH, Kador PF and Hotta N), pp. 72–81. Elsevier, Amsterdam, 1988.
13. Kador PF, Goosey JD, Sharpless NE, Kolish J and Miller DD, Stereospecific inhibition of aldose reductase. *Eur J Med Chem* **16**: 293–298, 1981.
14. Bradford MM, A rapid and sensitive method for the quantitation of microgram quantities of protein utilizing the principal of protein-dye binding. *Anal Biochem* **72**: 248–254, 1976.
15. Laemmli UK, Cleavage of structural proteins during the assembly of the head of bacteriophage T4. *Nature* **227**: 680–685, 1970.
16. Spackman DH, Stein WH and Moore S, Automatic recording apparatus for use in the chromatography of amino acis. *Anal Chem* **30**: 1190–1206, 1958.
17. Srivastava SK, Das B, Hair GA, Gracy RW, Awasthi S, Ansari SH and Petrash JM, Interrelationships among human aldose reductases: immunochemical, kinetic and structural properties. *Biochim Biophys Acta* **840**: 334–343, 1985.